TIME-RESOLVED SPECTROPHOTOMETRY OF THE AM HERCULIS SYSTEM E2003+225[1]

PATRICK MCCARTHY AND STUART BOWYER
Department of Astronomy and Space Sciences Laboratory, University of California, Berkeley

AND

JOHN T. CLARKE
Space Telescope Project and Space Science Laboratory, NASA Marshall Space Flight Center
Received 1985 October 4; accepted 1986 May 21

ABSTRACT

We present the results of time-resolved moderate resolution spectrophotometry of the AM Her type system E2003+225 over one complete orbital period. These observations were obtained when the continuum luminosity was 1.25–2 mag fainter than other recent observations, implying a significantly reduced rate of mass transfer. The photometric light curves of the emission lines and the 4860 Å continuum are similar, each showing sharp minima near linear polarization phases 0.5 and 1.0. The emission-line spectrum is dominated by a high-velocity broad component similar to that seen in other systems. Although we are unable to resolve the cores of these lines, this component has a velocity amplitude of ~ 500 km s^{-1} and in contrast to previously reported observations is symmetric at about zero velocity. The similarity between the light curves of this component and the 4860 Å continuum suggest that they arise in the same region. We propose that this emission arises from infalling material in the accretion stream. A number of other narrow emission-line components appear at various phases in the cycle. Some of these components have radial velocity behavior similar to that of the dominant high-velocity component, and we also ascribe this emission to gas in the accretion stream. We tentatively identify another component as arising from the heated face of the secondary. Finally, one particular emission-line component has a behavior that is very difficult to understand. This component appears as a set of stationary narrow emission lines displaced ~ 9 Å from their rest wavelengths and is seen most easily in the weak lines of He I. We discuss the possibility that this component results from linear Zeeman splitting of emission from material close to the primary.

Subject headings: stars: accretion — stars: binaries — stars: emission-line — stars: magnetic

I. INTRODUCTION

The number of known AM Her systems has increased rapidly in recent years due primarily to the optical identification of soft X-ray sources. The hallmark of these systems is their strong and variable polarization. Variations of linear and circular polarization with the orbital phase have been used as an important diagnostic for these systems and have led to a fairly clear picture of these objects. The basic model consists of a magnetic white dwarf primary accreting matter from a low-mass secondary onto one or both magnetic poles (see Liebert and Stockman 1985 for a review). Spectroscopy can play a crucial role in determining the location and physical conditions of various emitting regions.

One of the recently discovered AM Her systems is the *Einstein Observatory* X-ray source E2003+225. This source was shown to be a member of the AM Her class of variables by Nousek *et al.* (1982). Based on X-ray data, optical photometry, optical polarimetry, and low-resolution spectroscopy, Nousek *et al.* (1984), hereafter referred to as N84, have proposed a detailed picture of this system. The long orbital period of E2003+225 (at 222 minutes, it is the longest period yet known) makes it ideal for time-resolved spectroscopy. The long period also makes it particularly well-suited to a critical examination of the coupling between the gravitationally and magnetically channeled flow regions, as well as the synchronicity of the rotation of the primary with the orbital period.

[1] Based on observations performed at Lick Observatory, University of California.

We present time-resolved spectrophotometry for this source obtained when the source was 1.5–2 mag fainter than when observed by N84. We discuss our observing procedures in § II, our results in § III, the implications of these results in § IV, and summarize our conclusions in § V.

II. OBSERVATIONS AND DATA REDUCTION

The observations were made on 1984 June 24, using an image tube scanner on the Lick 3 m Shane Telescope (Robinson and Wampler 1972; Miller, Robinson, and Wampler 1976). The spectra were taken with a 800 line mm^{-1} grating in second order, giving 3.5 Å resolution in the wavelength range of 4000–5000 Å. Each integration was 4 minutes long and was simultaneous with a sky exposure in an adjacent aperture. The star minus sky exposures for each pair of observations were combined, giving 28 exposures of 8 minutes duration covering one complete 222 minute period. The standard stars BD+33°2642 and BD+28°4211, respectively, were observed immediately prior to and following the exposures of E2003+225. Exposures of He-Ar-Cd and Ne wavelength calibration lamps were also made prior to and following observations of the source, as were quartz lamp exposures.

All of the observations were made through a 4″ aperture in 2″–3″ seeing. Thus, we expect our absolute photometry to be good to $\sim 15\%$ with relative photometry from one exposure to the next being considerably better. The positions of our calibration lamp lines were measured to be stable to within 0.2 Å. The validity of our wavelength solution was verified by mea-

surements of the positions of the Balmer absorption lines in the standard stars.

III. RESULTS

a) Average Emission Spectrum

The average emission spectrum contains a mix of both high excitation lines such as He II 4686 and lines from low ionization species such as C II and H I. Our spectra show a flat and often inverted Balmer decrement and a strength for He II 4686 that sometimes exceeds that of Hβ. The optically thick Balmer lines characteristic of AM Her systems have generally been attributed to collisional processes between the $n = 2$ and higher levels, implying that the emitting regions have electron densities in excess of 10^{12} cm^{-3} (Stockman, Liebert, and Bond 1979).

In Table 1, we present the fluxes, equivalent widths, and full widths at half-maxima (FWHM) for the dominant lines at four points in the cycle. In Table 2, these measurements are shown for the sum of all the spectra over one complete period without any shifting of the wavelength arrays. The summed spectrum is shown in Figure 1. The continuum appears very flat in our spectra (in F_ν units), although the spectral range covered makes it difficult to derive an accurate power-law fit. Inverted Balmer decrements and flat continua in the red are characteristic of AM Her systems in the active state. The presence of a broad component in the emission and the lack of strong photospheric magnetic absorption features in the spectrum both argue against the system being in the canonical low state (e.g., Schneider and Young 1980) despite the fact that it was fainter by over 1.5 mag than during the 1982 observations of N84 and the 1984 July observations of Mukai *et al.* (1986).

b) Phasing

We have computed the time of zero linear polarization phase for our observations based on the ephemeris presented

TABLE 1
EMISSION-LINE PROPERTIES

Line	Wavelength	FWHM (Å)	Flux (ergs cm^2 s^{-1})
		Phase 0.246	
Hγ	4342.8	14.1	4.60×10^{-14}
He II	4687.6	09.3	4.01×10^{-14}
Hβ	4863.5	13.3	2.90×10^{-14}
He I	4473.7	16.3	9.04×10^{-15}
		Phase 0.517	
Hγ	4342.8	17.3	2.56×10^{-14}
He II	4689.7	11.6	1.83×10^{-14}
Hβ	4863.9	17.4	1.66×10^{-14}
He I	4474.7	13.5	5.57×10^{-15}
		Phase 0.736	
Hγ	4339.1	12.7	7.36×10^{-14}
He II	4684.0	9.2	3.61×10^{-14}
Hβ	4860.0	13.2	5.00×10^{-14}
He I	4470.7	8.2	1.68×10^{-14}
		Phase 0.991	
Hγ	4338.0	12.7	2.23×10^{-14}
He II	4682.1	14.7	2.34×10^{-14}
Hβ	4858.7	14.6	2.00×10^{-14}
He I	4469.7	15.5	5.76×10^{-15}

TABLE 2
EMISSION-LINE PARAMETERS FOR SUMMED SPECTRA

Line	Wavelength	FWHM (Å)	Flux (ergs cm^2 s^{-1})	EQW (Å)
Hγ	4341.1	17.0	5.43×10^{-14}	26.5
He II	4685.7	14.9	3.96×10^{-14}	28.7
Hβ	4860.9	17.6	3.89×10^{-14}	25.2
He I	4472.3	16.1	1.16×10^{-14}	7.5
He I	4922	...	3.93×10^{-15}	3.2
He I	4388	...	1.01×10^{-15}	0.6
He II/N III	4541/4640	...	4.53×10^{-15}	3.0
C III	4647	...	5.43×10^{-15}	3.5

by Osborne *et al.* (1986). The accuracy of this ephemeris leads to an uncertainty in the time zero phase at the epoch of our observations of 1–2 minutes. The agreement in the phasing between our observations and those of Mukai *et al.* (1986) is confirmed by the presence of photometric minima near phases 0.5 in both data sets and by the similar phasing of the center of light velocity curves of the emission lines in the spectra.

c) Photometry

We have measured the AB magnitude of the continuum at 4860 Å by fitting the continuum in two 50 Å bands on either side of Hβ. The integrated strengths of the Balmer lines and He II 4686 were determined by summing under the lines in each spectrum. The strength of Hβ and the continuum magnitude are plotted against linear polarization phase in Figures 2 and 3, respectively. For comparison with standard magnitudes, at phase 0.75 the AB_{4860} mag is 16.70, while the standard B mag is 16.21. The simplicity and similarity of these two curves strongly suggest that both the continuum and the bulk of the line emission arise in the same region. Both curves show smooth drops in flux at the onset of the continuum dim phase ($\phi = 0.5$–1.0) followed by a smooth rise and fall and end in a dramatic increase in flux at the end of the dim phase. The continuum varies by almost a factor of 2 in flux while the Balmer lines vary by more than a factor of 3. The minimum seen at phase 0.5 corresponds to the principle minimum seen at this phase by N84 while the second minimum at phase 1.0 corresponds to the very weak secondary minimum that they observed. The strong minimum at phase 0.5 was seen by N84 in all optical bands as well as in the soft X-rays. During the phase interval $\phi = 1.0$–0.5, the continuum and the lines show much less dramatic variations, with both gradually declining.

d) Emission-Line Components

We were able to identify a number of distinct components in our emission-line profiles with varying degrees of clarity. Profiles of Hβ from each of our spectra are shown in Figure 4. We fitted a sine curve of the form

$$V = \gamma + K \sin 2\pi(\omega t + \phi_0)$$

to the dominant narrow component for the lines He II 4686 and He I 4471. The Balmer lines were too confused to give a satisfactory fit by themselves. The radial velocity variations of He II 4686 and He I 4471 are shown in Figure 5 along with our sine curve fit.

The results of these fits yield velocity amplitudes, $K = 500 \pm 20$ km s^{-1}, a systemic velocity of $\gamma \leq 30$ km s^{-1} and phase lag of $\phi_0 \approx 0.23$. One obvious difference between
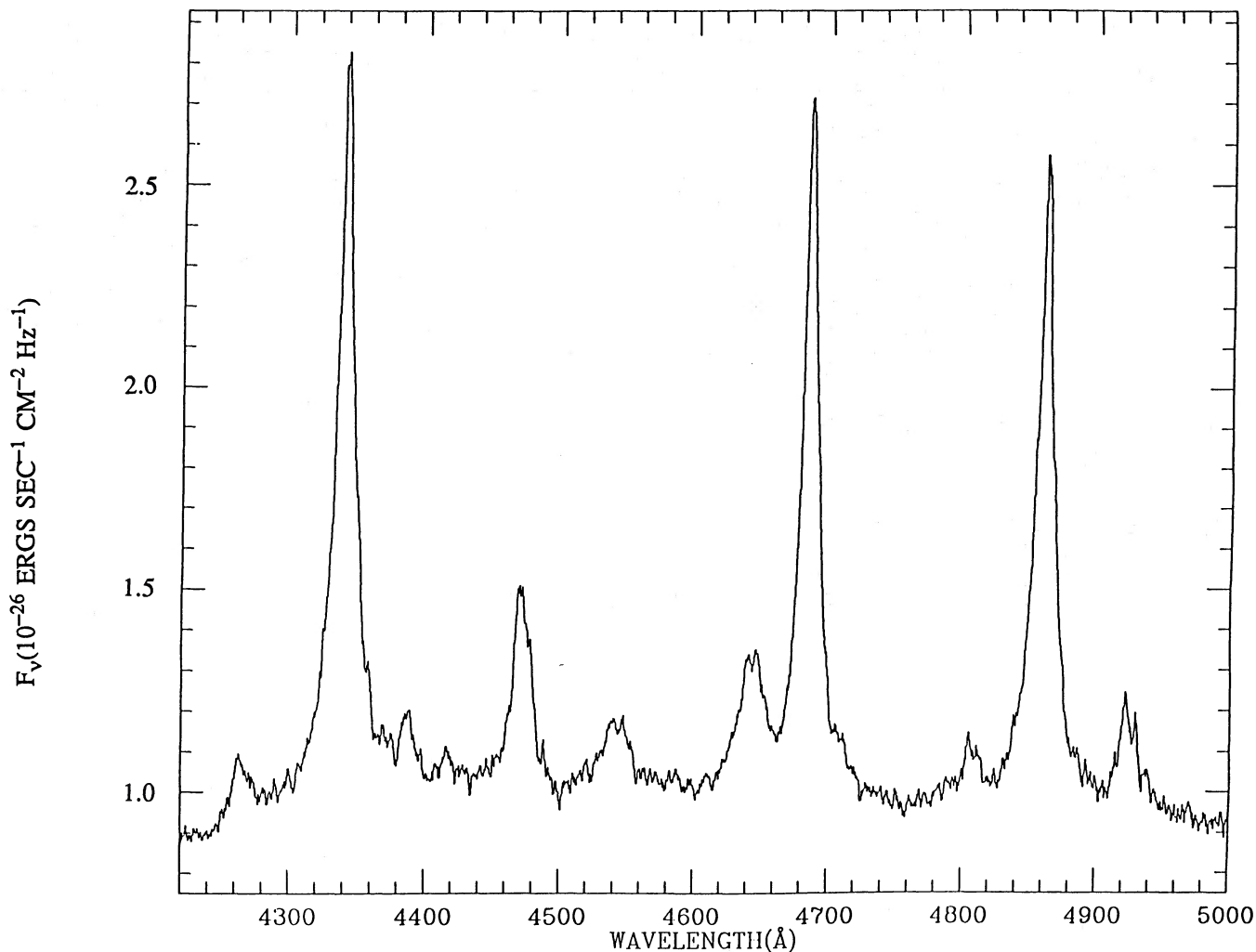
FIG. 1.—The sum of 28 spectra are shown covering one complete orbital period. No attempt has been made to shift the spectra in wavelength before addition.

our spectra and those of N84 is the small values of γ derived from our data. In the spectra presented by N84, the lines were redshifted throughout the entire orbital period, reaching nearly zero velocity at the time of minimum light.

Throughout the orbital cycle, the emission lines show a number of distinct components. Uniquely separating all of the components is quite difficult. One narrow component can be unambiguously identified throughout the entire cycle, except during the brief minima at phases 0.5 and 1.0. In this component the lines have a broad base and a narrow, unresolved core. They have an estimated width comparable to the spectral resolution of 250 km s^{-1} and show fast sinusoidal velocity variations (~ 500 km s^{-1}) throughout the cycle. Hereafter, we will refer to this component as the fast narrow component.

A number of other narrow emission-line components can be seen at various phases through the cycle. In the phase interval 0.5–0.85, a narrow (intrinsic FWHM = 220 km s^{-1}) component can be seen moving rapidly to the blue in all of the lines but most notably in He II 4686. This component has a similar K value to the fast narrow component but leads it in phase by 64°. This component then disappears from view as the fast narrow component dominates the spectrum. Another component is seen in all of the lines during the phase interval 0.85–0.1, but, in this case, it lags behind the fast narrow com-

ponent by 40°. At linear polarization phase 1.0, when the fast-moving components are suppressed, a narrow unresolved component at rest wavelength is visible. This component is visible only during a brief interval in the phase centered about the secondary minimum at phase 1.0.

The last emission line which we discuss here is highly unusual. Throughout the phase interval 1.0–0.5, there is a high-velocity narrow component that appears on the red wing of each line. This component is severely blended but detectable in the stronger lines (e.g., He II 4686) and is clearly resolved in the He I lines. The most interesting property of this component is that it shows no detectable velocity variations (≤ 150 km s^{-1}) during the phase interval 0.1–0.5. Furthermore, the velocity of this component appears to be different for lines of different excitation. In He I, the velocity is 500 km s^{-1}, whereas in Hβ it is 400 km s^{-1}. However, severe blending makes this measurement uncertain. It is possible that emission from Mg II 4481 at a blueshift of 170 km s^{-1} could be partly responsible for the feature seen to the red of He I 4471. We believe that this is unlikely, however, since Mg II λ4481 is weak in these systems and there is little evidence for a broad component to this line. Additionally, similar stationary redshifted lines appear in the other He I lines that are free from contamination. The lack of detectable velocity variations in this component is very difficult
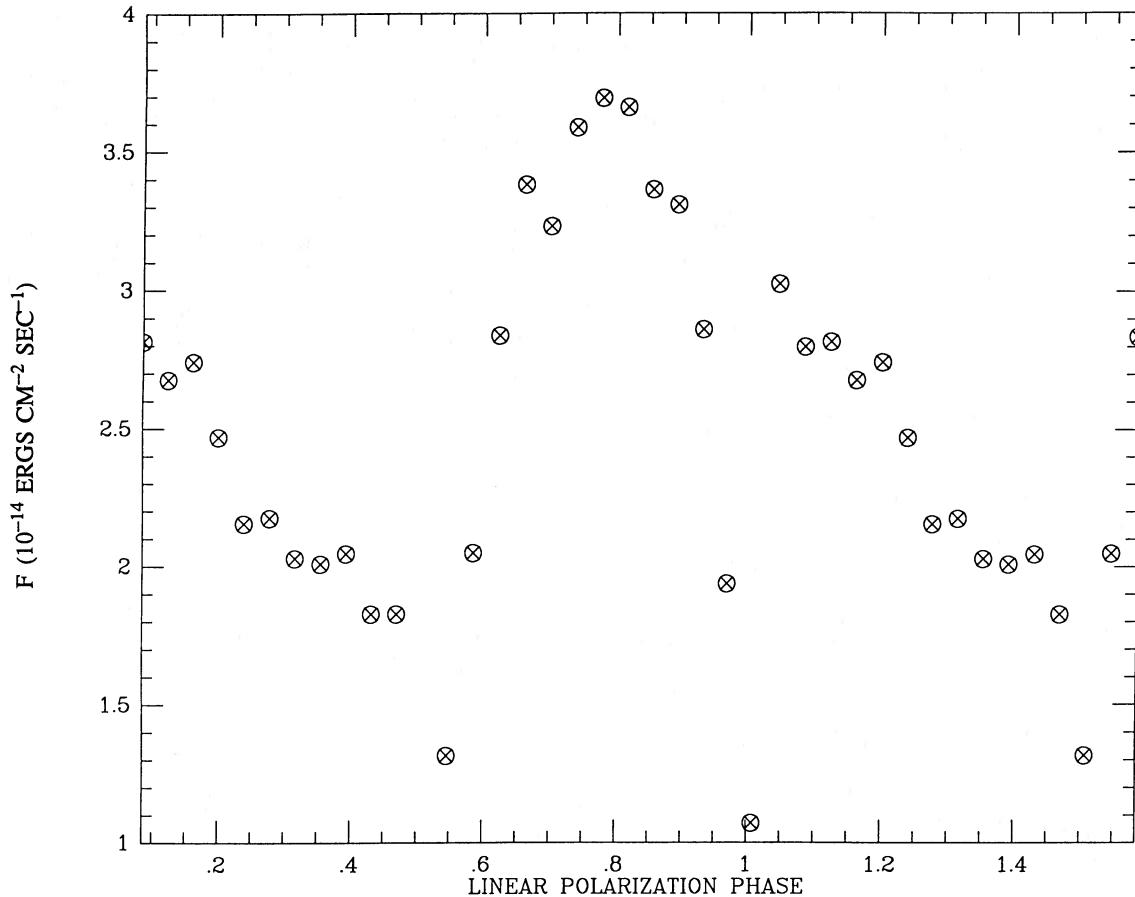
FIG. 2.—The integrated flux of Hβ is shown against linear polarization phase from the ephemeris of Osborne et al. (1986)

to understand from the standard view of the AM Her phenomenon.

In Figure 6, we have plotted the Hγ, He II 4686, and He I 4471 profiles as a function of phase for the interval from 0.97 to 0.16. These data demonstrate a number of important properties of this system. The narrow emission lines believed to be associated with the secondary at phase 1.0 are clearly delineated. The increase in line fluxes following the minimum at phase 1.0 is dramatic, and the line profiles also change at this point. The stationary lines in the He I 4471 can also be seen in this phase interval.

Finally, we have made a centroid of the lowest 10% of the flux in the strongest lines to measure the radial velocity behavior of the broad base component. The broad base shows a sine wave motion of similar amplitude, k, and system velocity, γ, as the fast narrow component but leads this component by ~ 0.15 in phase. The broad base may be interpreted as arising higher up in the curved accretion stream than the fast narrow component and is most likely associated with turbulence in the infall velocities at the kink in the accretion stream as described in the model of Liebert and Stockman (1985).

IV. DISCUSSION

We discuss the implications of our results in terms of the standard model of the AM Her phenomenon and, where possible, we refer to the more detailed picture recently put forward by Liebert and Stockman (1985). Following standard practice, we will assume that the rotation axis of the primary and the

orbital axis of the system are coincident. The geometry of the accreting pole is then specified by the system inclination i and the colatitude of the accreting pole Δ, and the phase lag $\Delta\Phi$ between the secondary and the accreting pole. Generally, one needs polarimetric data as well as photometry and spectroscopy to determine the relevant angles. Having only spectrophotometric data, we cannot precisely determine the inclination angle and the colatitude of the accreting pole. We can, however, place some constraints on the system orientation and infall velocities and extrapolate using the linear polarization ephemeris of N84.

The fast narrow component is qualitatively very similar to the fast narrow component seen in many other AM Her systems, e.g., VV Pup (Schneider and Young 1980). This component has generally been identified with the heated face of the secondary. In the two systems in which the secondary can be located unambiguously, E1114+182 (Biermann et al. 1985) and AM Her (Young and Schneider 1979; Young, Schneider, and Shectman 1981), the narrow emission lines do indeed locate the secondary. However, it is easily demonstrated that in this case the strongest narrow emission lines do not arise on the heated surface of the secondary. If one assumed that the radial velocity of the fast narrow emission lines reflects the motion of the secondary, then the high velocity of the fast narrow component and the long period of this system lead to a mass function for the white dwarf M_{wd} and the red dwarf M_{rd} $(M_{wd} + M_{rd}) \sin^{-3} i$, in excess of 2 $M_\odot$. This is clearly unrealistic for an AM Her system.
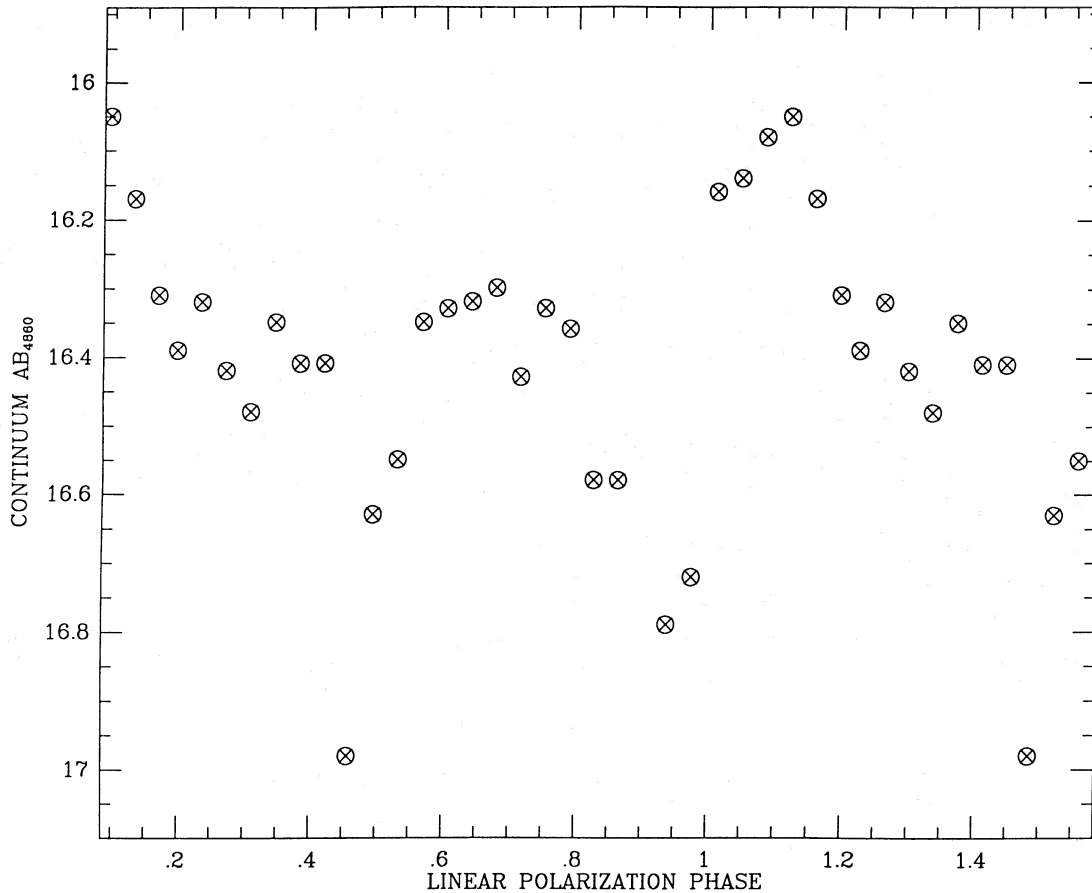
FIG. 3.—The continuum flux centered around Hβ is plotted against linear polarization phase as in Fig. 2

Another argument against this interpretation involves the maximum in the circular polarization observed by N84 at phase 0.5. Using the radial velocity of the fast narrow emission line to locate the secondary would require that it be at inferior conjunction near phase 0.75, thus placing it 90° out of phase with the accreting pole. While phase differences of up to 60° have been suggested for some systems, a phase lag of 90° is rather implausible. We suggest that the observed radial velocity variations of the fast narrow component are dominated by projected infall. This can explain the large velocity amplitude without resorting to unrealistically large masses. The fact that this component is at maximum redshift at the time of the primary eclipse indicates that the material giving rise to the emission is most likely located along a radial accretion column oriented along our line of sight at phases 0.5 and 1.0. This interpretation is consistent with the circular polarization data of N84. Their data show a maximum in circular polarization at phase 0.5. If the fast narrow component does arise from the lower part of the accretion column, then the fact that the maximum circular polarization and the maximum projected infall velocity occur at nearly the same phase indicates that the lower part of the accretion column points radially toward the accreting pole. The phase difference of 0.15 between the broad base and fast narrow components suggests that the kink in the accretion stream leads the magnetic pole by $\sim 50°$.

The true infall velocity may be deduced from the projected velocity given the inclination of the system, i, and the latitude of the accreting pole, Δ. For a radial accretion column, the infall velocity can be expressed as

$$V = V_{\text{observed}} \csc (i + \Delta) .$$

Using the values for i and Δ derived by N84, we find an infall velocity of ~ 700 km s^{-1}. The weak linear polarization pulse observed by N84 and used to define the time of zero linear polarization phase requires that the accretion column make a steep angle with the line of sight. In fact, N84 requires the column to be oriented at an angle of 70°–80° to the line of sight at the time of superior conjunction to explain both the line-integrated radial velocities and linear polarization measurements. Our spectroscopy shows the fast narrow component to be at maximum blueshift at this phase. This implies that the line-emitting material makes a small angle with the line of sight. This suggests that the emitting material may be distributed over a large region of the column during periods of reduced accretion.

The origin of the low-velocity narrow component seen near phase 1.0 is difficult to determine because of the limited resolution of the data and the brief amount of time that the component is visible. We can place an upper limit of ~ 180 km s^{-1} on the velocity amplitude of this component. If the system mass is typical of AM Her systems ($\sim 0.5\ M_{\odot}$), this amplitude is consistent with what one would expect from material located on the surface of the secondary star. The proposed explanation of the fast narrow component would suggest that the secondary is at superior conjunction near the time of the secondary minimum. The system orientation com-
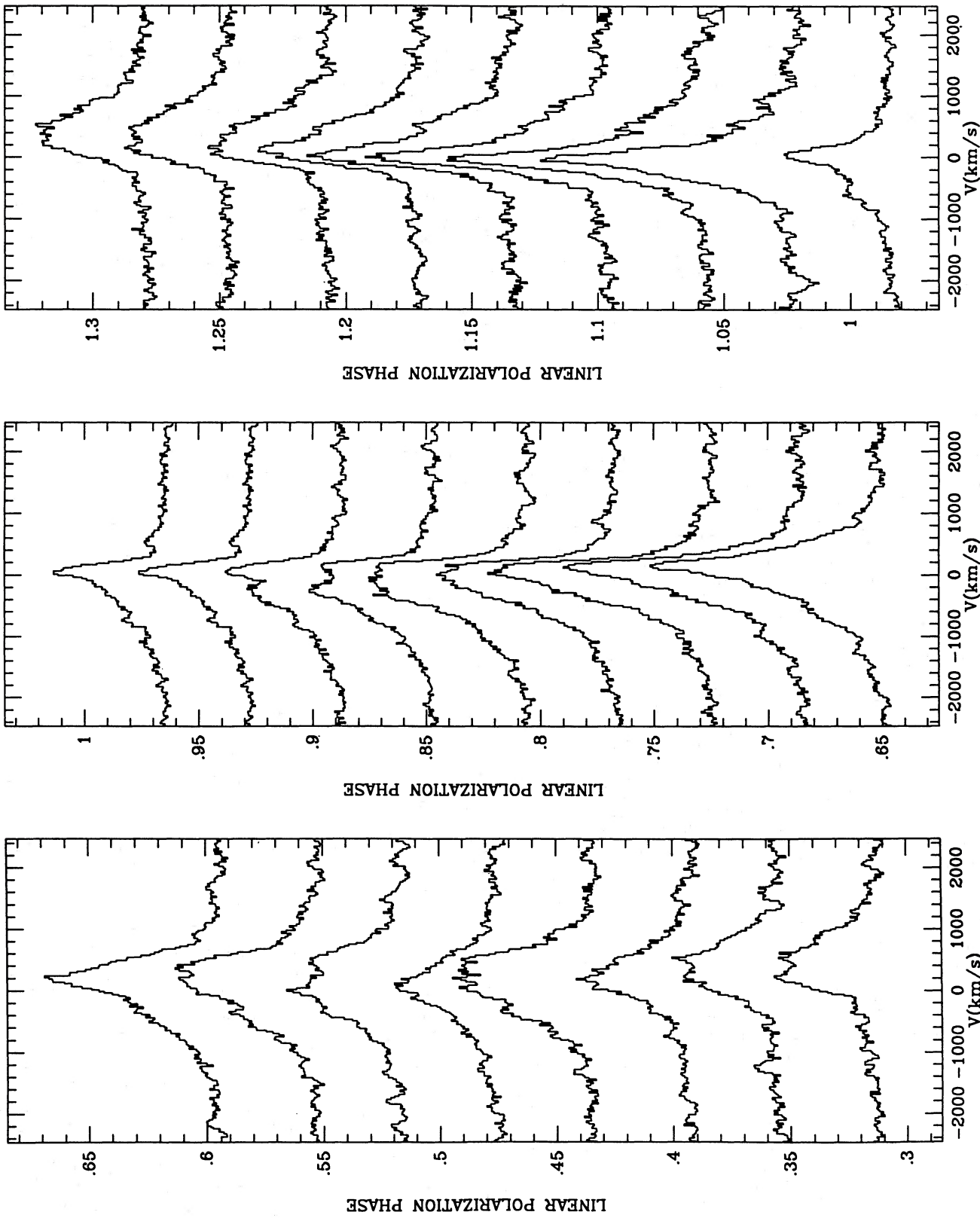
FIG. 4.—Profiles of Hβ are shown from each of our 28 spectra covering one complete orbital period. The ordinate is increasing linear polarization, and the abscissa is observed radial velocity. Each spectrum had a zero point shift added for display, but the relative intensities are preserved. The phase interval of 0.05 corresponds to a flux increment of 10^{-26} ergs cm^2 s^{-1} Hz^{-1}.
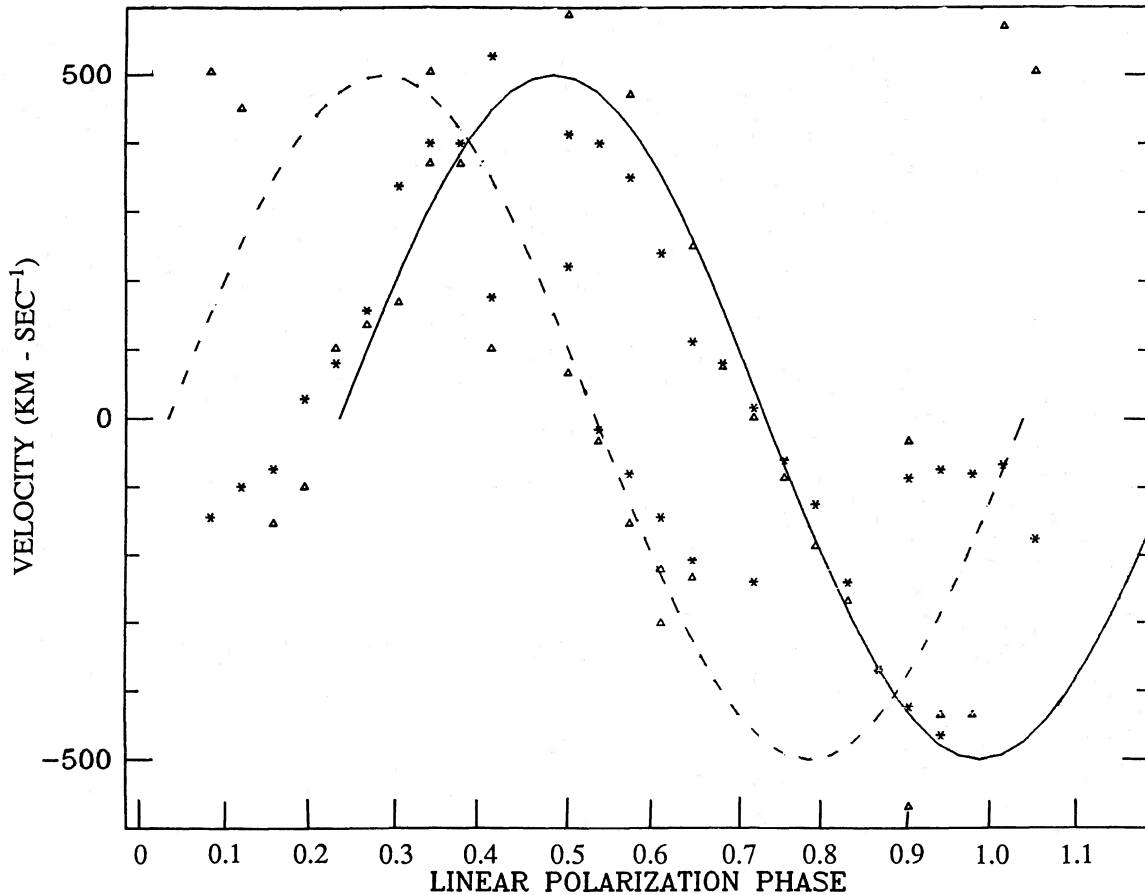
FIG. 5.—The radial velocities in kilometers per second of the dominant emission line components for He II 4686 (Δ) and He I 4471 (*) are plotted against linear polarization phase. Our fit to the fast narrow component is shown as a solid line, and our fit to the leading component (described in § IIId) is shown as a dotted line, with the constraint that this component has the same amplitude and period as the fast narrow component.

bined with the fact that the accretion region is obscured at this point in the cycle makes the conditions optimal for viewing the secondary. Although the brief time that the low-velocity component is visible makes it difficult to demonstrate conclusively that this emission arises from the heated face of the secondary, all of the evidence is consistent with this interpretation. From our measurement of fluxes of the narrow lines at phase 1.0, we can place limits on emission from the secondary at the levels listed in Table 3.

The short duration and large amplitude of the secondary minimum are not only quite different from that seen by N84 but are also hard to reconcile with their picture in which the accretion column just barely grazes the limb. The depth of the eclipses is ∼0.7 mag in the continuum, about a factor of 3 in the lines, and is total in the X-ray observations of N84, thus

TABLE 3

SECONDARY EMISSION LIMITS

Emission Line	Flux[a]
Hβ	4.30
Hγ	4.30
He II 4686	4.36
He I 4471	0.87
He I 4921	0.78

[a] 10^{-15} ergs cm^2 s^{-1}.

suggesting that the column is optically thick in the continuum and perhaps in the lines as well. The linear polarization pulse observed by N84 at phase 1.0 rules out the possibility of the primary eclipsing the column at this time. Self-eclipsing by the column is plausible but requires a rather large degree of curvature and a fairly uniform brightness distribution along the column. This is because the infalling matter is behind the cyclotron region at phase 1.0. The observed dip in the light curve would then imply a fairly uniform brightness distribution along the column. We suggest that this is, in fact, the case and that the enhanced secondary minimum seen in our observations results from a more uniform distribution of light along the column at times of reduced accretion.

The last narrow emission lines we discuss are the highest velocity component of the system, the apparently stationary component seen most strikingly in the lines of neutral helium. This component is clearly seen during the phase interval 1.0–0.5 at a velocity of 500 km s^{-1} in He I 4471. This component is also easily seen in the summed spectrum in Figure 4 with all of the weaker lines showing a peak to the red of the rest wavelength. A weaker component also appears to be present during this phase interval at −500 km s^{-1}. Throughout this phase interval, these components show no detectable systematic motion, although the blue component is often very weak. A full half-phase later, at phase 0.25, this component is also seen strongly in He I, *still* at +500 km s^{-1}. The fact that all of

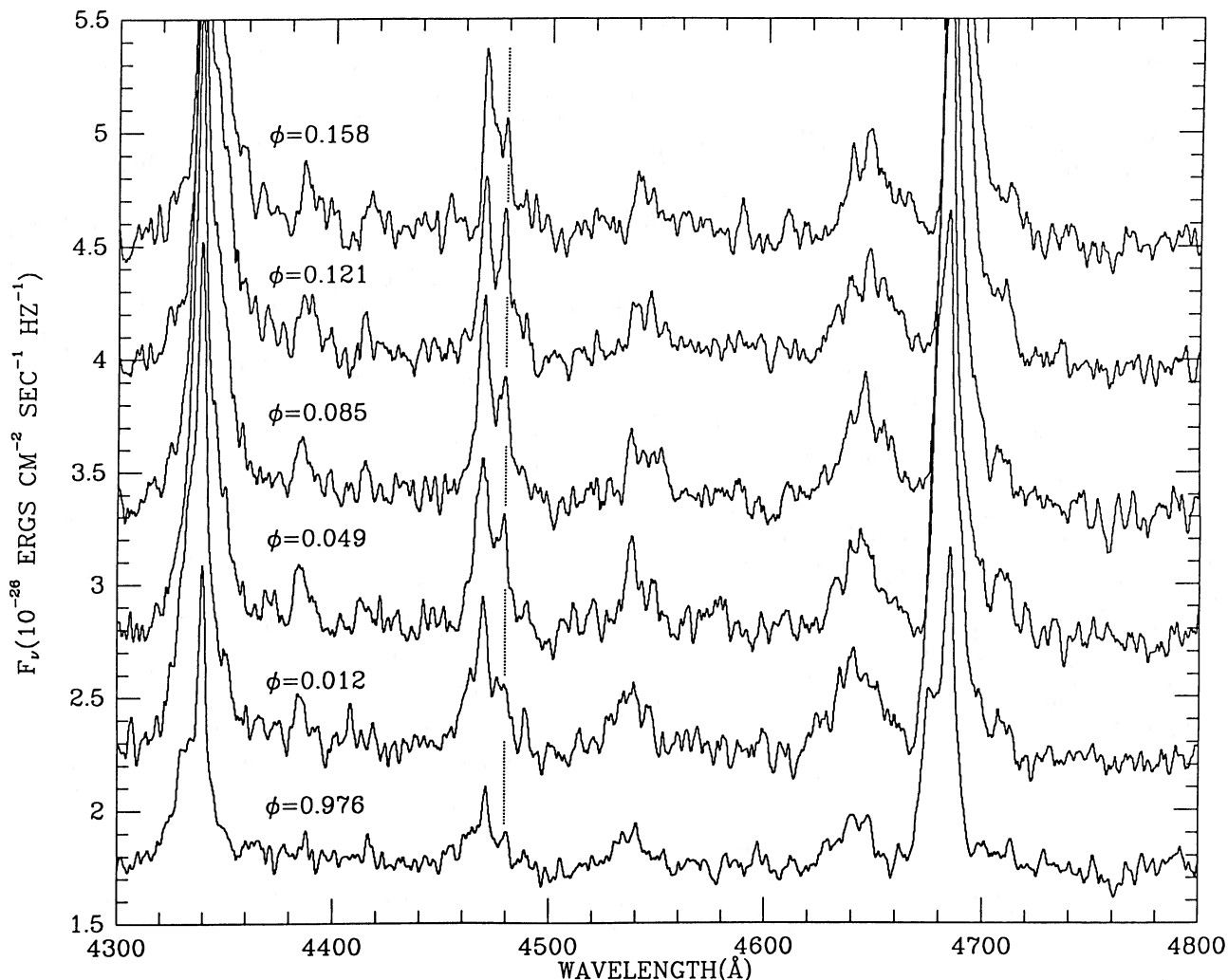FIG. 6.—The profiles Hγ, He II 4686 and He I 4471 are shown plotted against phase for the interval from 0.97 to 0.16. The stationary lines of He I 4471 are indicated by a vertical dotted line.

the other components are near zero velocity makes it easy to see this component at this time. Thus, it appears that there is a narrow emission-line component at a velocity of $+500$ km s^{-1} throughout the entire cycle as well as (possibly) a weaker component at a velocity of approximately -500 km s^{-1}. These components show no detectable periodic motion. The fact that this component is absent during the eclipse at phase 1.0, when the white dwarf is on the far side of the system, clearly demonstrates that the material responsible for this emission is located very close to the primary. The lack of detectable orbital motion in these lines also implies that the emission originates from near the center of mass of the system.

All of these properties are consistent with what one would expect from Zeeman split emission lines arising from a region, e.g., a shock front, located near the primary. In a shock front located above the surface of the primary, one would expect field strengths of several hundred kilogauss to a few megagauss. The location of such a region near the primary could well render the radial velocity variations undetectable with the resolution of these observations. We have considered this explanation for the stationary lines in E2003+225. To test this hypothesis, one must compare the ratio of splitting of lines arising from the same lower level of a single ion. Different ionic species will recombine at different distances behind the accretion shock and will experience different field strengths. Unfortunately, for this purpose, we have only the lines of neutral helium available. The Balmer lines of hydrogen are badly blended and confused with the other components previously discussed, and the red wing of Hγ is contaminated by Hg 4358 emission from the San Jose sky. We have measured the wavelengths of the stationary lines of He I 4471 and He I 4921. The measurements for He I 5015 are too uncertain since this line falls near the end of our spectral range and is dominated by noise. The wavelength shifts of these lines in the summed spectrum are $+7$ Å, -8 Å and $+8.5$ Å, -6.8 Å, respectively.

Theoretical line profiles for H I and He I for strong fields have been calculated by Kemic (1974) and Surmelian and O'Connell (1974). The increase in splitting with decreasing energy for a given series of lines is supported by our data but at a low level of confidence. The fields strength implied from our measurements is ~ 1 mG, but it is not strongly constrained. Using this value and assuming a dipole field configuration and a surface field of 30 mG, as is typical of AM primaries (Liebert and Stockman 1985), the implied height of the emitting region

above the surface is a few white dwarf radii, which is quite reasonable. The observed narrow profiles of the lines requires that the radial extent of the emitting region be quite small, on the order of a few tenths of a white dwarf radius. Emission from a thin ring of material, or a torus, would produce a similar spectrum, but such a system would be inherently unstable in fields of the strength expected near the primary. This is precisely why Am Her systems differ from accreting binary systems containing disks. Thus, while we cannot definitely prove the stationary lines are the result of Zeeman splitting, this explanation is suggested by and consistent with the available data.

Finally, we address the differences between the system in 1982 as observed by N84 and our recent observations. The principal differences are the reduced overall brightness of the system at the time of our observations, the asymmetry between the two minima in the 1982 light curve, and the differences in the velocity curves of the emission lines. The wealth of emission line components in our spectra are a result of our higher resolution and the higher signal-to-noise ratio of our spectra. The reduced overall brightness of the system at the time of our observations implies a reduced accretion rate. Our light curve for the 4680 Å continuum is similar to the U-band light curve of N84 except for the difference in the relative strength of the two minima.

The difference in the velocity curves of the lines in these two observations seems inconsistent with real changes in systematic velocity. While we can explain the different amplitudes as being due to differing techniques of measurement and a varying rate of accretion, we are unable to offer any convincing model that will explain the difference of ~ 500 km s^{-1} in the zero points of the velocity curves. That our velocity curve is correct for the epoch of our observations is supported by the observations performed one month following our observations by Mukai $et\ al.$ (1985), who find a similar systemic velocity. We note, moreover, that Osborne $et\ al.$ (1986) obtain a systemic velocity of -350 ± 120 km s^{-1} from a low-resolution spectrum. This result is marginally consistent with our results but is totally inconsistent with N84.

V. SUMMARY

We have presented time resolved spectrophotometry of the AM Her binary E2003+225 over one complete orbital period. The similarity between the light curves of the lines and the continuum strongly argues that both arise in the same region. These observations of the longest period AM Her system known have allowed us to critically test some of the long-held beliefs concerning these systems, most notably the validity of using the dominant narrow emission-line component to locate the secondary.

The case for the dominant narrow emission not locating the secondary is quite strong for this system. Our observations suggest that the source of the dominant narrow emission lines is material undergoing collimated radial infall in the accretion column. This interpretation implies infall velocities on the order of 500 km s^{-1}. The long period of this system provides a natural explanation of the lack of strong emission from the secondary. The large separation between the two components results in suppression of reprocessed light compared to emission from the accreting regions. The two sharp minima in the light curves of the lines and continuum are proposed to be the result of self-eclipsing of the accretion stream. The multiplicity of fast moving narrow emission-line components implies a complex geometry in the accretion stream. Finally, we have observed an apparently stationary set of narrow emission-line components with velocities on the order of 500 km s^{-1}. We suggest that this emission may be the result of linear Zeeman splitting of emission from material close to the primary. If Zeeman splitting is the source of these lines, then the implied field strength of 1 mG appears to be quite reasonable, given the current state of knowledge regarding the surface fields of AM Her primaries.

REFERENCES

Biermann, P., $et\ al.$ 1985, $Ap.\ J.$, **293**, 303.
Kemic, S. B. 1974, $Ap.\ J.$, **193**, 213.
Liebert, J., and Stockman, H. S. 1985, $Cataclysmic\ Variables\ and\ Low\ Mass$ X-$Ray\ Binaries$, ed. J. Patterson and D. Q. Lamb (Cambridge, Mass.: Reidel).
Miller, J. S., Robinson, L. B., and Wampler, E. J. 1976, $Advances\ in\ Electronics$ $and\ Electron\ Physics$, **40B**, 693.
Mukai, K., $et\ al.$ 1986, $M.N.R.A.S.$, in press.
Nousek, J. A., Luppino, G., Gajar, S., Bond, H., Grauer, A., Schmidt, G., Hill, G., and Tapia, S. 1982, $IAU\ Circ.$ No. 3733.

Nousek, J. A., $et\ al.$ 1984, $Ap.\ J.$, **277**, 682 (N84).
Osborne, J., $et\ al.$ 1986, $M.N.R.A.S.$, in press.
Robinson, L. B., and Wampler, E. J. 1972, $Pub.\ A.S.P.$, **84**, 161.
Schneider, D. P., and Young, P. 1980, $Ap.\ J.$, **238**, 946.
Stockman, D. P., Liebert, J., and Bond, H. E. 1979, in $IAU\ Colloquium\ 53,$ $White\ Dwarfs\ and\ Variable\ Degenerate\ Stars$, ed. H. M. Van Horn and V. Weidemann (Rochester: University of Rochester Press), p. 334.
Surmelian, G. L., and O'Connell, R. F. 1974, $Ap.\ J.$, **193**, 705.
Young, P., and Schneider, D. P. 1979, $Ap.\ J.$, **230**, 502.
Young, P., Schneider, D. P., and Shectman, S. A. 1981, $Ap.\ J.$, **245**, 1043.

STUART BOWYER: Department of Astronomy, University of California, Berkeley, CA   94720

JOHN T. CLARKE: Goddard Space Flight Center, Mail Code 681, Greenbelt, MD   20771

PATRICK J. McCARTHY: Department of Astronomy, University of California, Berkeley, CA   94720